



Supporting Information

for *Small*, DOI: 10.1002/smll.202007610

Ultraprecision Imaging and Manipulation of Plasmonic Nanostructures by Integrated Nanoscopic Correction

*Yunbo Liu, Zhijia Zhang, Younggeun Park, and Somin Eunice Lee**

Supporting Information: Ultraprecision imaging and manipulation of plasmonic nanostructures by integrated nanoscopic correction (iNC)

Yunbo Liu, Zhijia Zhang, Younggeun Park, Somin Eunice Lee

Sample preparation

For nanomanipulation and nano-imaging, gold nanorods (30 nm x 100 nm) were synthesized as previously described^[1]. CTAC–AuNRs were synthesized by bromide-free seed-mediated growth. CTAC was replaced with PEG by round trip phase transfer. For comparison of nanoimaging and scanning electron microscopy, gold nanorods were fabricated using electron beam lithography on a glass substrate (Fig. S1). A 100 nm thick 950k A2 PMMA photoresist was first spin-coated onto a glass slide, followed by Ni beads drop-cast on the edge of the substrate to aid focusing in the e-beam process. Gold nanorods (50 nm x 110 nm) were then patterned using e-beam lithography (Jeol 6300FS) of varying distances and orientations. The sample was then developed and covered with 30 nm of gold using ebeam evaporation (Enerjet). A lift-off process was subsequently performed using acetone to dissolve the photoresist and form the nanorods on the glass substrate.

For nanoimaging, single gold nanorods were also conjugated to a self-assembled monolayer (SAM)^[2,3]. The glass slide was first baked in the oven at 60 °C for 16 h. After baking, the slide was subsequently plasma treated for 30 seconds before immersing in 1.64% 3-Aminopropyl triethoxysilane (APTES)/ethanol solution. After incubating in APTES solution for 24 hours, the slide was washed with ethanol five times and baked in the oven at 120 °C for 3 h. After baking, the slide was transferred into a gold nanorod solution (plasmon resonance wavelength: 802 nm) prepared by adding 1 mL gold nanorod solution (absorbance of 1) into 17.5

mL of DI water. The substrate was subsequently incubated in the nanorod solution for 12 h before washing with DI water to remove excess gold nanorods.

iNC

The iNC was constructed by adapting^[4] for integrated nanoimaging and nanomanipulation. To characterize the relation between the phase retardation and the applied voltage, the iNC was mounted after a linear polarizer LP (Fig. S3). Beam was generated by a 660nm laser (Newport LPM660-60C) and collected by a power meter (Thorlabs PM400 and S130C). Function generator was used to apply a voltage signal to the iNC. To determine θ_0 , with no voltage applied, the LP was rotated to where the minimum transmission power was measured. The LP was rotated in 5° increments (θ_n). At each increment, the applied voltage was adjusted to where the minimum transmission power was measured.

To operate the iNC in the polarizer mode, the iNC was placed after a fixed linear polarizer LP (Fig. S4). White light was generated and collected by a spectrometer (Ocean Optics USB2000+) at each wavelength. A 2 kHz square wave signal was generated by a function generator (Instek AFG-2225) to LC_1 and LC_2 of the iNC. Both V_{LC1} (3.05V to 11.9 V) and V_{LC2} (3.58V to 11.6V) were tuned synchronously from -90 degrees to 90 degrees in 5 degree increments. The resulting intensity change was recorded by the spectrometer at various wavelengths from 630 nm to 690 nm. To characterize the time response of the iNC in the polarizer mode, the iNC was placed after a fixed linear polarizer (Fig. S5). Both V_{LC1} and V_{LC2} were given a turn-on voltage of 3V and 3.3V respectively lasting 200 ms at the same time. Beam was generated by a 660nm laser (Newport LPM660-60C). The resulting output response was acquired using a quadrant position detector QPD and a DAQ board (NI PCI6733).

To characterize the iNC in the power modulator mode, the iNC was placed after a fixed linear polarizer and before a spectrometer (Ocean Optics USB2000+) (Fig. S9). The transmitted light was coupled into the spectrometer through an optical fiber. A 2 kHz square wave signal was generated by a function generator (Instek AFG-2225) to LC1 and LC2 of the iNC. V_{LC1} was tuned from 3V to 5.5 V while V_{LC2} was held constant at 3.3V, which corresponded to changing the transmission power from minimum to maximum. The linear region ranged from 3.8V to 4.8V. The power intensity at each wavelength λ from 630 nm to 690 nm was then recorded and normalized. To characterize the temporal response of the iNC in the power modulator mode, the iNC was placed after a fixed linear polarizer (Fig. S11). V_{LC1} was given a turn-on voltage of 3V lasting 200 ms while V_{LC2} was kept on at 3.3V. Beam was generated by a 660nm laser (Newport LPM660-60C). The resulting output response was acquired using a quadrant position detector QPD and a DAQ board (NI PCI6733).

To operate the iNC in the polarization rotation mode, the iNC was placed between two linear polarizers LPs to analyze the transmission light polarization direction (Fig. S10). V_{LC2} was tuned from 3.3V to 11.4 V while V_{LC1} was held constant at 3V to change the transmission polarization direction from -90 degrees to 90 degrees in 5 degree increments. The transmission light intensity was analyzed by a spectrometer at different wavelengths λ from 630 nm to 690 nm. The resulting polarization direction ξ was then determined through sinusoidal fitting. To characterize the temporal response of the iNC in the polarization rotator mode, the iNC was placed between two linear polarizers LPs (Fig. S12). V_{LC2} was given a turn-on voltage 3.3V lasting 200 ms while V_{LC1} was kept constant at 3V. Beam was generated by a 660nm laser (Newport LPM660-60C). The resulting output response was acquired using a quadrant position detector QPD and a DAQ board (NI PCI6733).

Nanoimaging analysis

The normalized root-mean-square deviation (RMSD) of nano-images was calculated for each pixel^[5]. Nano-images obtained using a conventional polarizer were spatially corrected down to 0.1 pixel accuracy by first interpolating the raw images using the nearest neighbor method, and then translating based on the amount of shift detected between each image. Nano-images obtained using the iNC were not spatially corrected. In both cases, the normalized RMSD for the pixel (m , n) was calculated as

$$\text{RMSD}(m,n) = \frac{1}{I_{e,\max}(m,n) - I_{e,\min}(m,n)} \sqrt{\frac{\sum_{i=1}^N (I_{e,i}(m,n) - I_{s,i}(m,n))^2}{N}}, \quad (\text{S1})$$

where N is the number of frames (each frame is taken at one polarization direction), I_e is the experimental value of the intensity, I_s is the theoretical value fitted to a sinusoidal functions, and $I_{e,\max}$ and $I_{e,\min}$ are the maximum and minimum intensity at pixel (m , n) over all polarization directions, respectively.

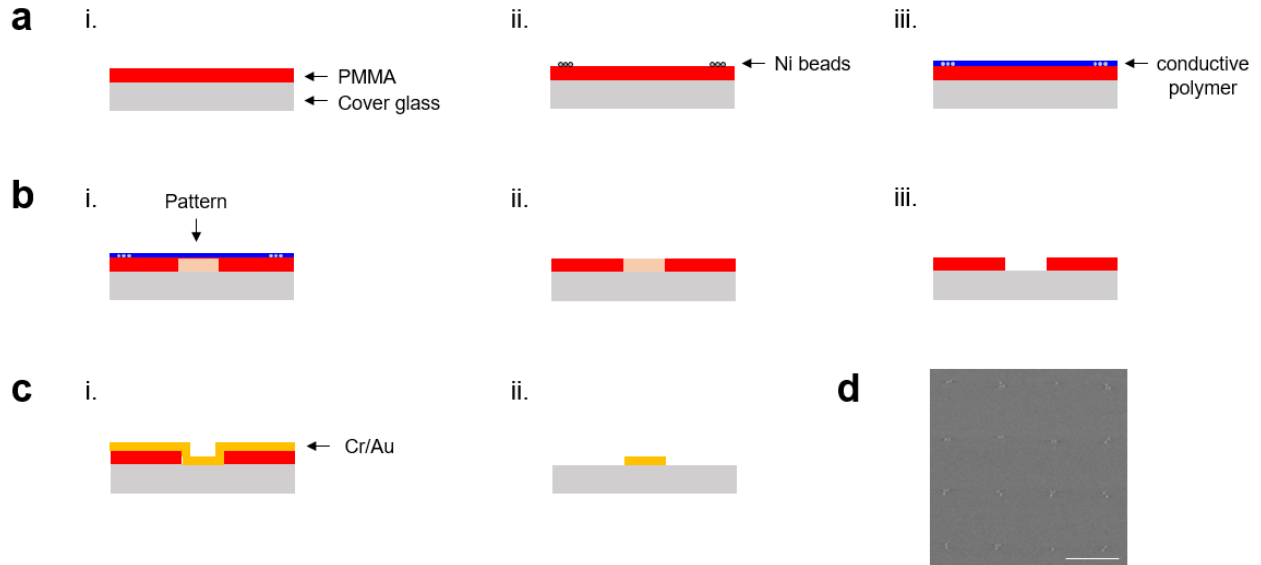


Figure S1. Fabrication process. (a) A 100 nm thick 950k A2 PMMA photoresist was first spin-coated onto a glass slide, followed by Ni beads drop-cast on the edge of the substrate to aid focusing in the e-beam process. A conductive polymer was then spin-coated onto the substrate to avoid e-beam charging of the surface. (b) Gold nanorods were then patterned using ebeam lithography (Jeol 6300FS). The sample was then developed. (c) The sample was then covered with 2 nm of Cr and 40 nm of gold using ebeam evaporation. A lift-off process was subsequently performed using acetone to dissolve the photoresist, resulting in the final nanorods on the glass substrate. (d) Scanning electron microscopy image. Scale bar: 2.5 μm .

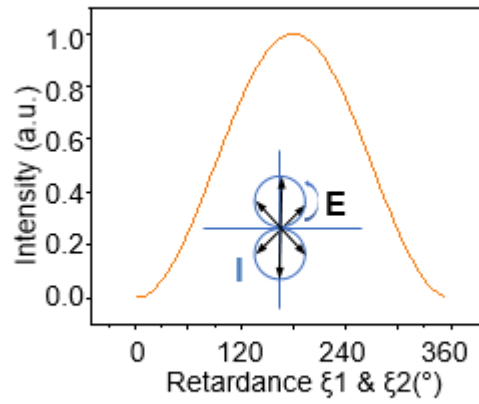


Figure S2. Theoretical simulation of iNC in the polarizer mode following Eq. (1) and (2).

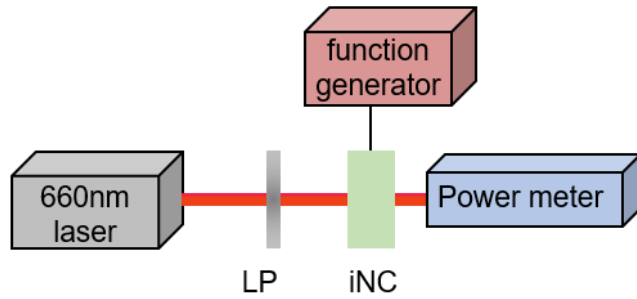


Figure S3. Experimental setup for characterizing phase retardation as a function of applied voltage. Optical path consisted of a linear polarizer LP and the iNC. Beam was generated using a 660nm laser. Power meter was used to measure the output light intensity. Applied voltage levels, to control the iNC, were generated using a function generator.

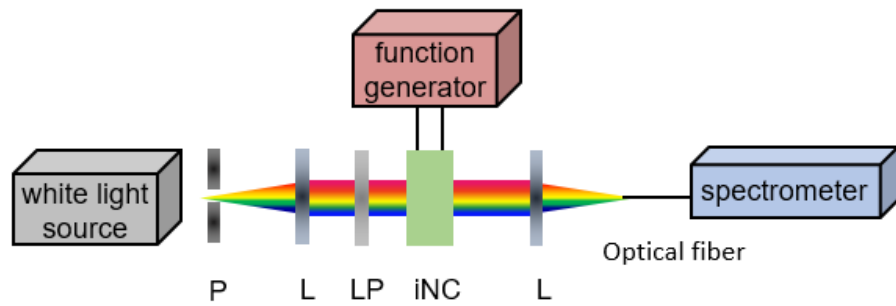


Figure S4. Experimental setup for characterizing the iNC in the polarizer mode. Optical path consisted of an iris diaphragm P, convex lens L, linear polarizer LP, iNC, and another convex lens L. Applied voltage levels to control the iNC were generated using a function generator. L was used to collimate white light and another L was used to couple light into a spectrometer.

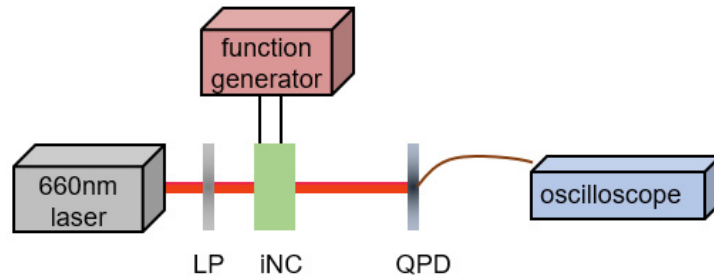


Figure S5. Experimental setup for characterizing the time response of the iNC in the polarizer mode. Optical path consists of a linear polarizer LP, iNC, and quadrant position detector QPD. Beam was generated using a 660 nm laser. QPD was connected to an oscilloscope for data acquisition.

	d (nm)	ℓ (nm)
Fig. 3d ii, right	310	310
Fig. 3d iii, left	274	274
Fig. 3d iii, right	218	217
Fig. 3d iv, left	201	206
Fig. 3d iv, right	131	131

Figure S6. Comparison of distance d by the iNC versus distance ℓ measured by SEM.

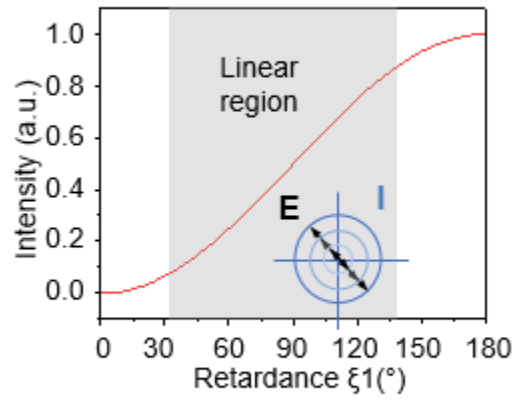


Figure S7. Theoretical simulation of the iNC in the power modulator mode following Eq. (3) and (4).

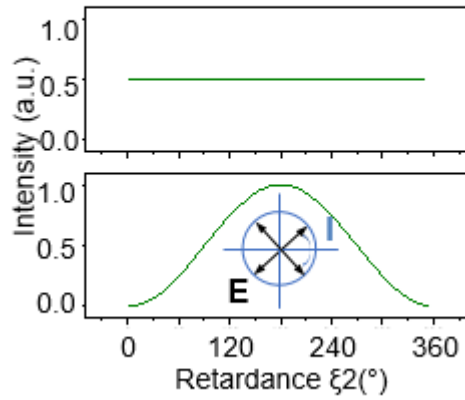


Figure S8. Theoretical simulation of the iNC in the polarization rotator mode following Eq. (5) and (6). The transmission intensity is kept at a constant $\frac{1}{2}$ as shown (top). The polarization state of the transmission light is rotated with respect to the retardance of LC₂ (δ_2) (bottom).

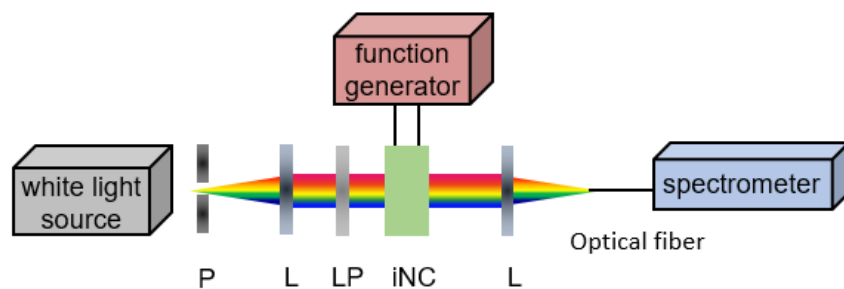


Figure S9. Experimental setup for characterizing the iNC in the power modulator mode.

Optical path consisted of an iris diaphragm P, convex lens L, linear polarizer LP, iNC, and another convex lens L. Applied voltage levels to control the iNC were generated using a function generator. L was used to collimate white light and another L was used to couple light into a spectrometer.

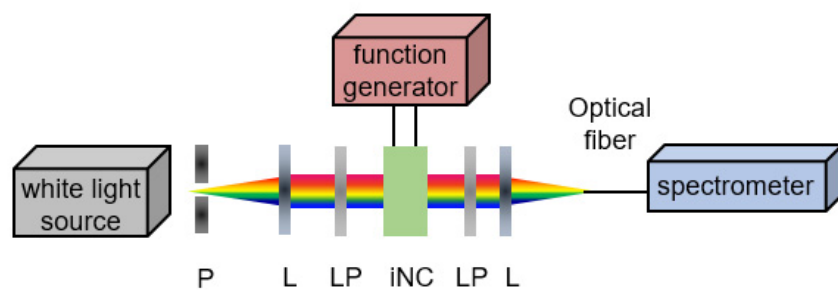


Figure S10. Experimental setup for characterizing the iNC in the polarization rotator mode.

Optical path consisted of an iris diaphragm P, convex lens L, linear polarizer LP, iNC, LP, and L.

Applied voltage levels to control the iNC were generated using a function generator. L was used

to collimate white light and another L was used to couple light into a spectrometer.

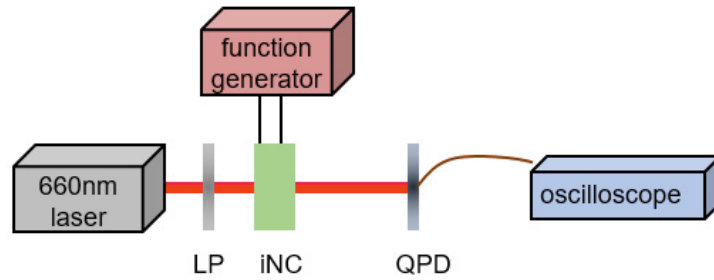


Figure S11. Experimental setup for characterizing the time response of the iNC in the power modulator mode. Optical path consists of a linear polarizer LP, iNC, and quadrant position detector QPD. Beam was generated using a 660nm laser. QPD was connected to an oscilloscope for data acquisition.

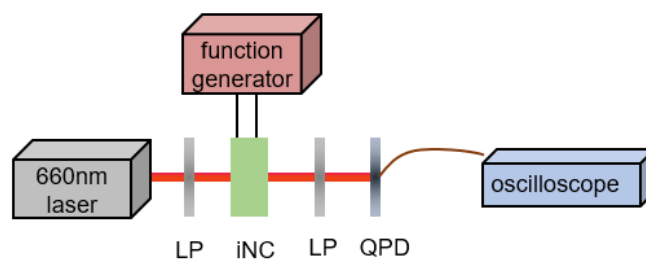


Figure S12. Experimental setup for characterizing the time response of the iNC in the polarization rotator mode. Optical path consists of a linear polarizer LP, iNC, LP, and quadrant position detector QPD. Beam was generated using a 660nm laser. QPD was connected to an oscilloscope for data acquisition.

Supporting References

- [1] W. K. Lin, G. Cui, Z. Burns, X. Zhao, Y. Liu, Z. Zhang, Y. Wang, X. Ye, Y. Park, S. E. Lee, *Adv. Mater. Interfaces* **2021**, *8*, 1.
- [2] C. Cao, S. Birtwell, J. Høgberg, H. Morgan, A. Wolff, D. Bang, *Diagnostics* **2012**, *2*, 72.
- [3] A. Sarkar, T. Daniels-Race, *Nanomaterials* **2013**, *3*, 272.
- [4] A. Safrani, I. Abdulhalim, *Opt. Lett.* **2009**, *34*, 1801.
- [5] Y. Liu, Y. Wang, S. E. Lee, *Proc. SPIE* **2018**, *10506*, 1.